Fluorescence Tomography and the Generalized Attenuated Radon Transform Under Capricorn

Alvaro R. De Pierro,
University of Campinas, Applied Mathematics Department,
Brazil

IPUC, Florianópolis, September 2011

Work by

- Eduardo Xavier Miqueles, IMECC-UNICAMP *

[0]* Supported by FAPESP grant No 09/15844-4, Brazil
[0]* Supported by CNPq grant No 476825/2006-0, Brazil

Work by

- Eduardo Xavier Miqueles, IMECC-UNICAMP *
- ARDP **

0* Supported by FAPESP grant No 09/15844-4, Brazil
0* Supported by CNPq grant No 476825/2006-0, Brazil

Work by

- Eduardo Xavier Miqueles, IMECC-UNICAMP *
- ARDP **

Thanks to the Nuclear Instrumentation Laboratory (Federal University of Rio de Janeiro), Brazil, and the Brazilian Synchrotron Light Laboratory (LNLS), that provided the real data.

Articles: Physics in Medicine & Biology, 55 (2010), IEEE Transactions on Medical Imaging, 30, 2, (2011), Studies in Applied Mathematics, to appear , Computer Physics Communications, to appear, http://www.ime.unicamp.br/∼milab (software and papers).

[0]* Supported by FAPESP grant No 09/15844-4, Brazil
[0]* Supported by CNPq grant No 476825/2006-0, Brazil

The Problem and the Model

The Problem and the Data

- We want to reconstruct the concentration distribution of a heavy metal (Copper, Zinc, Iron,..), or other element like Iodine, inside a body.

The Problem and the Data

- We want to reconstruct the concentration distribution of a heavy metal (Copper, Zinc, Iron,..), or other element like Iodine, inside a body.
- This concentration distribution could indicate malignancy in a tissue, for example. Another application is determination of 3D rock structure in mineralogy.

The Problem and the Data

- We want to reconstruct the concentration distribution of a heavy metal (Copper, Zinc, Iron,..), or other element like Iodine, inside a body.
- This concentration distribution could indicate malignancy in a tissue, for example. Another application is determination of 3D rock structure in mineralogy.
- Irradiation by high intensity monochromatic synchrotron X rays at a specific energy of the element stimulates fluorescence emission (data).

The Synchrotron

The Synchrotron: Data Acquisition

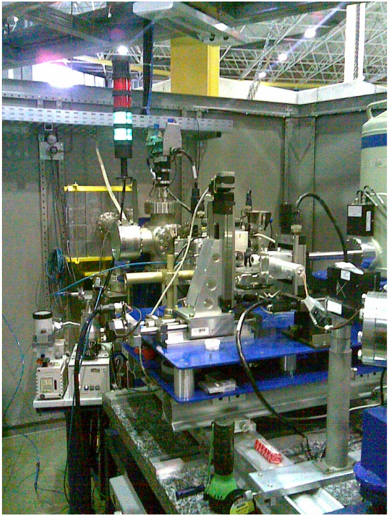

Inside a synchrotron gate

X-Rays Fluorescence Computed Tomography (XFCT)

Aims at reconstructing fluorescence emitted by the body when bombarded by high intensity X-rays at a given energy.

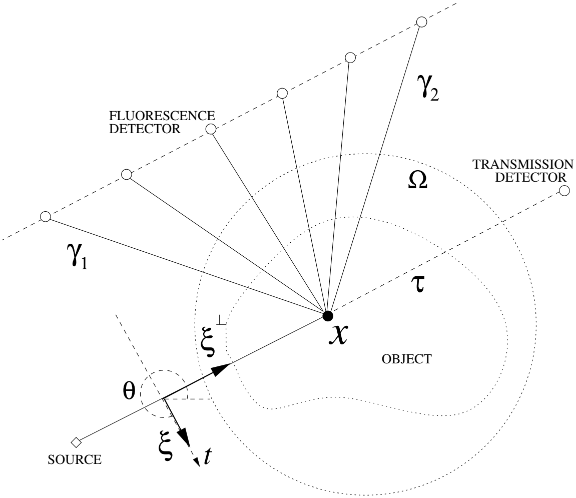

The Generalized Attenuated Radon Transform

And the model is

$$d(t,\theta) = \mathscr{R}_W f(t,\theta) = \int_{x\cdot\xi=t} f(x)W(x,\theta)dx$$

where $f(x)$ is the emission (fluorescence) density at x, μ is the fluorescence attenuation, λ is the attenuation of the X-rays,

$$W(x,\theta) = \omega_\lambda(x,\theta)\omega_\mu(x,\theta),$$

$$\omega_\mu(x,\theta) = \int_\Gamma e^{-\mathscr{D}\mu(x,\theta+\gamma)}d\gamma \text{ , and}$$

$$\omega_\lambda(x,\theta) = e^{-\mathscr{D}\lambda(x,\theta+\pi)},\ \mathscr{D}h(x,\theta) = \int_{\mathbb{R}} h(x+q\xi^\perp)dq$$

What do we know?: CT and SPECT

X-Rays Computed Tomography (CT)

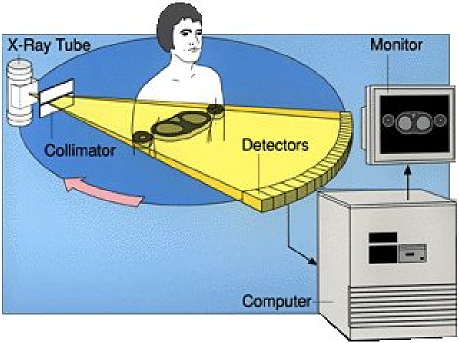

CT data collection

SPECT Scanner

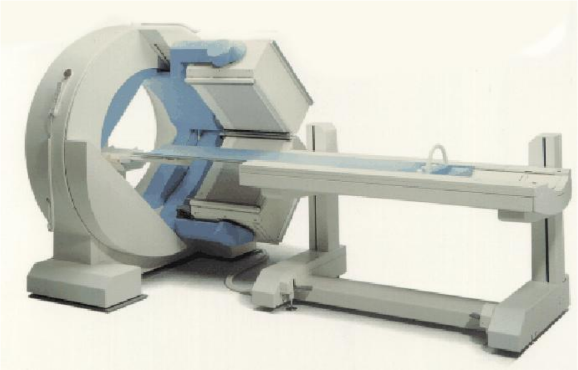

SPECT Scanner

Detection

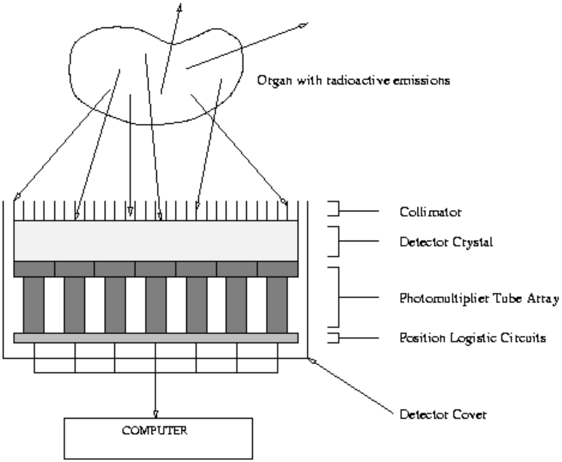

SPECT detection

SPECT= Single Photon Emission Computed Tomography, aims at reconstructing a tagged process inside the body, for example, blood flow tagged with T^{99}.

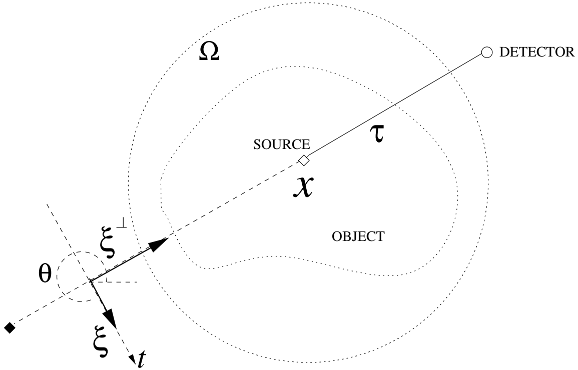

SPECT geometry

Mathematically

If no attenuation is considered, the Radon Transform is the model for both problems (CT and SPECT)

$$d(t,\theta) = \mathcal{R}f(t,\theta) = \int_{x\cdot\xi=t} f(x)dx$$

where $(t,\theta) \in [-1,1] \times (0,2\pi)$, $\xi = \xi(\theta)$ is a direction vector defined by an angle θ, $\xi = (\cos\theta, \sin\theta)$ and $\xi^{\perp}$ is such that $\xi \cdot \xi^{\perp}=0$

The Projection Theorem and the Inversion of the Radon Transform

$$\mathcal{R}^{-1} = \mathcal{F}_2^{-1} \mathcal{F}_1$$

where $\mathcal{F}_2$ and $\mathcal{F}_1$ stand for the two and one dimensional Fourier Transforms.

The Attenuated Radon Transform

But photons could be absorbed !!!!!!!!!!!!!!!!!!!!

$$d(t,\theta) = \mathbb{R}_{\omega} f(t,\theta) = \int_{x\cdot\xi=t} f(x)\omega_{\mu}(x,\theta)dx$$

where μ is the attenuation, and

$$\omega_{\mu}(x,\theta) = e^{-\mathscr{D}\mu(x,\theta)}$$

where, as before, $\mathscr{D}h(x,\theta) = \int_{\mathbb{R}} h(x+q\xi^{\perp})dq$

No Projection Theorem !!!!!!!!!!!

The Inversion of $\mathcal{R}_\omega$

Alternatives:

- Discretize and solve an optimization model. Too computationally intensive (hours for a single reconstruction if we regularize). Not our option.

The Inversion of $\mathcal{R}_\omega$

Alternatives:

- Discretize and solve an optimization model. Too computationally intensive (hours for a single reconstruction if we regularize). Not our option.
- Approximate by a scaled Radon Inverse and Iterate.

The Inversion of $\mathcal{R}_\omega$

Alternatives:

- Discretize and solve an optimization model. Too computationally intensive (hours for a single reconstruction if we regularize). Not our option.
- Approximate by a scaled Radon Inverse and Iterate.
- Try to find an analytic inverse, but how?, what direction?

Iterative Inversion

First Option: Iterated Inversion

We have a reasonable (fast, accurate if there is not too much noise) inverse for $\mathscr{R}$, so, let us try a fixed point iteration !!!!

$$f^{(k+1)} = f^{(k)} + e^{(k)} =$$

$$(I - \frac{1}{a}\mathscr{R}^{-1}\mathscr{R}_W)f^{(k)} + \frac{\mathscr{R}^{-1}}{a}d,$$

$$e^{(k)} = \frac{\mathscr{R}^{-1}\left(d - \mathscr{R}_W f^{(k)}\right)}{a}$$

And what is a?

Iterated Inversion

Clearly, convergence depends on how close $\frac{1}{a}\mathscr{R}^{-1}\mathscr{R}_W$ is to the identity, equivalently, how well $\mathscr{R}^{-1}$ approximates $\mathscr{R}_W^{-1}$ and this depends on the attenuation. If it is too large, it will not work. To compensate for that, Chang (IEEE TNS 78) suggested for SPECT a reasonable value for a is the average attenuation given by

$$a(x) = \frac{1}{2\pi}\int_0^{2\pi} W(x,\theta)d\theta.$$

A Contraction Constant

The Contraction constant for

$$\mathcal{K}f = \frac{1}{a}\left(\mathscr{R}^{-1}(\mathscr{R} - \mathscr{R}_W)f - (1-a)f\right) = f - \frac{1}{a}\mathscr{R}^{-1}\mathscr{R}_W f \quad (1)$$

is given by

$$\mathbf{c}(\kappa_a) = \sup_{\mathbf{u}\in\mathbb{R}^2} \sup_{\theta\in[0,2\pi]} \left| 1 - \frac{1}{2\|a\|_\infty}\left[W(\mathbf{u},\theta) + W(\mathbf{u},\theta+\pi)\right] \right| \quad (2)$$

And

Sequences $\mathbf{c}(\kappa)$ and $\mathbf{c}(\kappa_a)$ for different (increasing) values of attenuation μ, meaning that, we have a reasonable computable value measuring convergence rate and ill-conditioning.

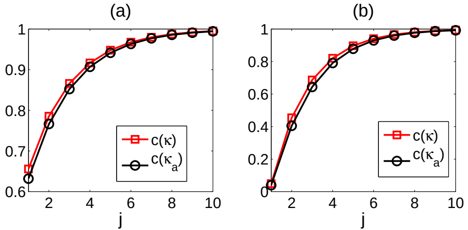

Classical Methods in a Continuous Setting: EM

The Expectation Maximization (EM) can also be applied to the linear part of our problem, assuming a known attenuation function. For the EM we have the following iteration (continuous version):

$$f^{(k+1)}(x) = f^{(k)}(x)\frac{\mathscr{B}_W d^{(k)}(x)}{\mathscr{B}_W e(x)},$$

where $d^{(k)}(t,\theta) = d(t,\theta)/\mathscr{R}_W f^{(k)}(t,\theta)$, $\mathscr{B}_W d(x) = \int_0^{2\pi} W(x,\theta)d(x\cdot\xi,\theta)d\theta$ is the attenuated backprojection, and $e = 1$ in **V**.

Unknown Attenuation: Iteration Once Again

New Problem: *Given* $d \in \mathbf{V}$, *find* $\{f, \mu\} \in \mathbf{U}$ *such that*

$$\mathcal{Y}(f, \mu) = \mathscr{R}_{W(\mu)} f - d = 0 \in \mathbf{V}. \quad (3)$$

Iterate:

$$f^{(k+1)} = \mathbf{L}\left(d, f^{(k)}, \mu^{(k)}\right), \qquad \mu^{(k+1)} = \mathbf{N}\left(d, f^{(k+1)}, \mu^{(k)}\right).$$

L stands for an approximate inversion of $\mathscr{R}_W$ given $\mu^{(k)}$ and **N** for the application of (say) Newton‘s method to equation (1) for $f^{(k+1)}$ given.

Some Experiments: Simulated Data

Figure below shows a 32x32 representation of functions $\{f, \mu, \lambda\}$ and the simulated attenuated Radon transform with 80 projections views and 60 rays per view.

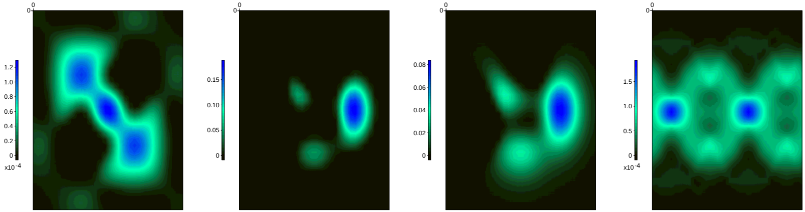

Simulated data for XFCT. From left to right: density function f, fluorescence attenuation μ, transmission attenuation λ and attenuated Radon transform.

Some Experiments: Real Data

A microscopic sample with a distribution of Copper and Zinc inside. For the Copper sample, each projection view had 23 rays, while 20 rays for the Zinc sample. The total number of views was 60 for both samples. Figure below shows the functions $\{\mathscr{R}\mu, \mathscr{R}_W f\}$.

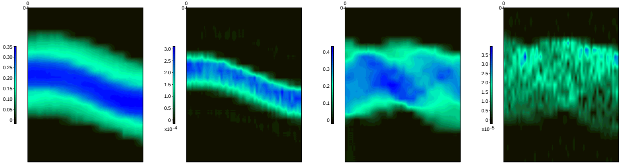

Real data. From left to right: transmission data for Cu sample, XFCT data for Cu sample, transmission data for Zn sample and XFCT data for Zn sample.

AKT $\times$ EM with $\mu = \lambda$ and for iterations $\{1, 2, 3, 4, 20\}$ (left to right). For each block, the EM reconstruction is shown in the first row and the AKT reconstruction in the second. Simulated case (32x32)

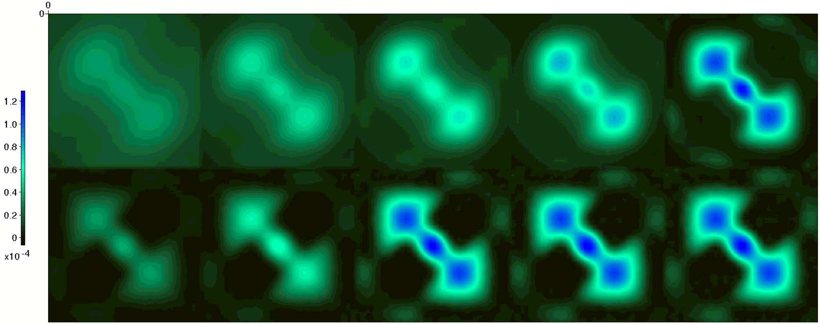

(a)

Some Experiments: Real Data

AKT × EM with $\mu = \lambda$ and for iterations $\{1, 2, 3, 4, 20\}$ (left to right). For each block, the EM reconstruction is shown in the first row and the AKT reconstruction in the second. Cu sample (60x60)

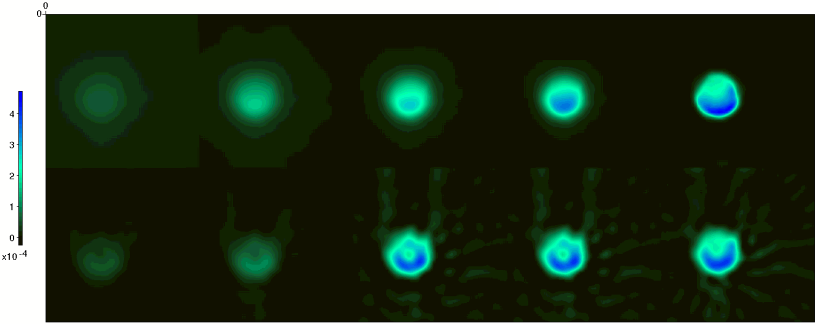

(b)

Some Experiments: Real Data

AKT $\times$ EM with $\mu = \lambda$ and for iterations $\{1, 2, 3, 4, 20\}$ (left to right). For each block, the EM reconstruction is shown in the first row and the AKT reconstruction in the second. Zn sample (60x60).

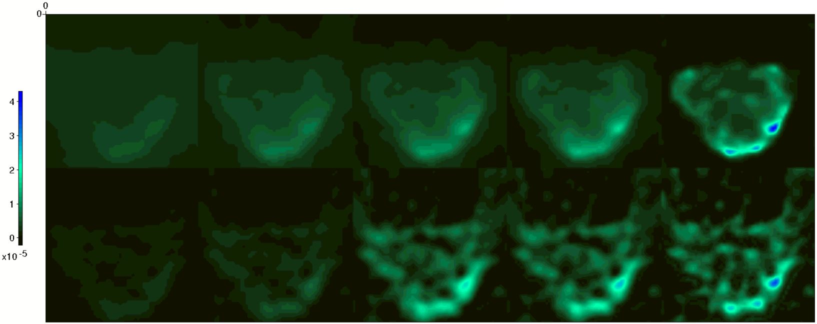

(c)

Some Experiments: Simulated and Real Data

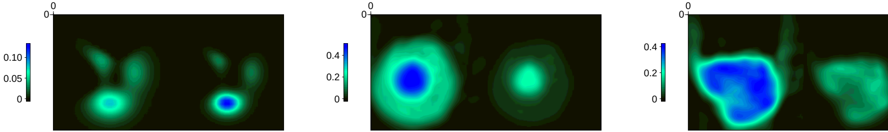

Iterates $\{\mu^{(0)}, \mu^{(1)}\}$, for AV, using AKT for $f^{(1)}$. Initial guess $\mu^{(0)}$ was obtained using FBP of transmission data.

An Analytic Inverse

Another Coincidence: Notices of the AMS, november 2005

About the Cover

A new Radon transform algorithm

This month's cover was suggested by the article of Fokas and Sung in this issue. In an article mentioned there, Fokas, Iserle and Marinakis describe a new algorithm for computing inverse Radon transforms, which I used to approximate the inverse transform of a simulated X-ray of the well-known head model—traditionally called *phantom*—of Logan and Shepp. For the non-expert, what is striking about such calculations is the odd mixture of science and rough guess that goes into them, made necessary by the awkward fit between the Radon transform and discrete approximation. Also the somewhat scary feeling involved in dealing even with phantom tumors.

—Bill Casselman, Graphics Editor
(notices-covers@ams.org)

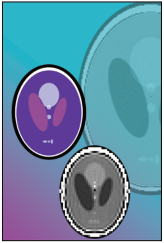

An Analytic Inverse

Following Fokas, the spectral analysis of the differential equation:

$$\eta \cdot \nabla u(x) + a(x, \eta) u(x) = f(x)$$

$\eta = \eta(\kappa) \in \mathbb{C}^2$, $\kappa \in \mathbb{C}$.

allows us to to write the solution in terms of the GART. $a = 0$ leads to the Radon Transform, $a(x) = \mu(x)$ to the Attenuated Radon Transform and $a(x, \eta)$ will be determined for the XFCT. In our case

$$\eta(\kappa) = \left[\frac{1}{2i} \left(\frac{1}{\kappa} + \kappa \right), \frac{1}{2} \left(\frac{1}{\kappa} - \kappa \right) \right]. \tag{4}$$

$\|\eta\| = o(\kappa)$ and each component of η is analytic in κ with a pole in zero.

An Analytic Inverse

Changing variables $x \mapsto (z, \bar{z})$, with $z \in \mathbb{C}$, defined by $z = v \cdot x$ and $v = v(\kappa) \in \mathbb{C}^2$.

$$\begin{pmatrix} z \\ \bar{z} \end{pmatrix} = Gx, \quad G = \begin{pmatrix} v^T \\ \bar{v}^T \end{pmatrix}, \quad \mathbf{J} = \begin{pmatrix} 0 & -1 \\ 1 & 0 \end{pmatrix} \tag{5}$$

The previous equation can be rewriten as

$$(\eta \cdot v)\partial_z u + (\eta \cdot \bar{v})\partial_{\bar{z}} u + a(x)u(x) = f(x). \tag{6}$$

An Analytic Inverse

We choose vector $\{\eta, v\} \in C^2$ such that $\eta \cdot v = 0$ and $\eta \cdot \bar{v} = j(\lambda) = \det G = -v \cdot \mathbf{J}\bar{v}$. Put $v = -\mathbf{J}\eta$ and denote $\eta(\kappa) = (c(\kappa), b(\kappa))^T$, then

$$j(\kappa) = c(\kappa)\overline{b(\kappa)} - b(\kappa)\overline{c(\kappa)} = 2iJ(\kappa), \quad J(\kappa) = \text{Imag}\left[c(\kappa)\overline{b(\kappa)}\right]. \tag{7}$$

Choosing η and v so that $\eta \cdot v = 0$ and $\eta \cdot \bar{v} = j(\kappa)$ we get

$$j(\kappa)\partial_{\bar{z}} u + a(x, \eta)u(x) = f(x).$$

An Analytic Inverse

Multiplying by an Euler factor $e^{q(x)}$ we decouple the equation obtaining two *d-bar* equations

$$\partial_{\bar{z}} \left(u(x) e^{q(x)} \right) = \frac{f(x)}{j(\kappa)} e^{q(x)}, \quad \partial_{\bar{z}} q(x) = \frac{a(x)}{j(\kappa)}$$

Define the singularity set $S = \{\kappa \in \mathbb{C} : \ j(\kappa) = 0\}$

An Analytic Inverse

And we can use for each equation the following (Fokas-Iserles, J.R.Soc.Interface, 3, 45-54, 2006.),

Lemma

For all $\kappa \notin S$, the solution of the $\partial_{\bar{z}} \hat{u}(x) = g(x)/j(\kappa)$ is given by

$$\hat{u}(x;\kappa) \doteq \partial_{\bar{z}}^{-1}\left(\frac{g(x)}{j(\kappa)}\right) = \frac{\alpha(\kappa)}{2\pi i}\int_{\mathbb{R}^2} \frac{g(y)dy}{v(\kappa)\cdot(y-x)}.$$

$\alpha(\kappa) = sign\ J(\eta)$.

for $g(x) = \frac{f(x)}{j(\kappa)}e^{q(x)}$ or $g(x) = \frac{a(x)}{j(\kappa)}$.

A Riemann-Hilbert problem

What is a scalar inhomogeneous Riemann-Hilbert (RH) problem?
Given a closed contour S and Hölder continuous functions f and g

on S, find a sectionally analytic function Φ with finite degree at infinity ($\Phi(z) \sim c_m z^m + O(z^{m-1})$ as $z \to \infty$, $c_m \neq 0$, $z \notin S$) such that

$$\Phi^+(t) = g(t)\Phi^-(t) + f(t)$$

In our case $g(t) = 1$.

An Analytic Inverse: a Riemann-Hilbert problem

S determines a curve, dividing the complex plane into two regions R^+ and R^-, where *d-bar* equations determine $u^\pm$ for $\kappa \in R^\pm$. The solution for all κ is determined by the jump $\mathcal{J}(x) = u^+(x) - u^-(x)$ on the curve S. Since u is an analytic function of $\kappa \notin S$, there exist $z_0 \in \mathbb{C}$ and $\delta > 0$ such that S is homotopic to a circle centered at z_0 and radius δ. Assuming without loss of generality that $\delta = 1$, the solution of our Riemann-Hilbert problem is given by (Ablowitz)

$$\begin{aligned} u(x;\kappa) &= \frac{1}{2\pi i}\int_{|z-z_0|=1} \frac{\mathcal{J}(x)}{z-\kappa}dz \\ &= \frac{1}{2\pi}\int_0^{2\pi} \mathcal{J}(x)e^{i\theta}\left\{\frac{-1}{\kappa} + O\left(\frac{1}{\kappa^2}\right)\right\}d\theta \\ &= \frac{1}{\kappa}h(x) + O\left(\frac{1}{\kappa^2}\right), \quad h(x) = \frac{-1}{2\pi}\int_0^{2\pi} \mathcal{J}(x)e^{i\theta}d\theta \end{aligned}$$

An Analytic Inverse

Therefore, from the original equation, and with the boundary condition $u(x) = O(\kappa^{-1})$ as $\kappa \to \infty$, we have

$$f(x) = \frac{1}{\kappa}\eta(\kappa) \cdot \nabla h(x) + a(x)O\left(\frac{1}{\kappa}\right) + O\left(\frac{1}{\kappa^2}\right), \quad \kappa \to \infty$$

It only remains to compute the jump function $\mathcal{J} = \mathcal{J}(x)$ in order to evaluate h in the above equation. And after many, many, ..., many, too many, ... calculations ....

http://onlinelibrary.wiley.com/doi/10.1111/j.1467-9590.2011.00527.x/abstract

An Analytic Inverse

$$f(x) = \frac{1}{2\pi}\int_0^{2\pi} i\mathbf{O}(\eta,\xi_\theta)\left[e^{\mathcal{D}a(x,\theta)} m\{\mathscr{R}a, \mathscr{R}_W f\}(x\cdot\xi_\theta,\theta)\right] d\theta \quad (8)$$

$$\doteq \mathcal{I}_\eta \mathscr{R}_W f(x) \quad (9)$$

giving rise to the inverse operator $\mathcal{I}_\eta$. Where

$$m\{r,d\} = e^{-\frac{r}{2}}\left\{h_c(r)\mathscr{H}\left(h_c(r)e^{\frac{r}{2}}d\right) + h_s(r)\mathscr{H}\left(h_s(r)e^{\frac{r}{2}}d\right)\right\} \quad (10)$$

where $h_c(r) = \cos(\frac{1}{2}\mathscr{H}r)$ and $h_s(r) = \sin(\frac{1}{2}\mathscr{H}r)$, and

$$\mathbf{O}(\eta,\xi_\theta) = [\mathbf{D}(\eta)\xi_\theta]\cdot\nabla - i[\mathbf{D}(\eta)\xi_\theta^\perp]\cdot\nabla \quad (11)$$

and matrix $\mathbf{D}(\eta) = \mathrm{diag}\left(\eta_1(\kappa)/\kappa, i\eta_2(\kappa)/\kappa\right)$.

An Analytic Inverse

Better

$$f(x) = \frac{1}{4\pi} \int_0^{2\pi} \partial_t \left[e^{\mathcal{D}a(x,\theta)} m\{\mathscr{R}a, \mathscr{R}_W f\} \right] (x\cdot\xi_\theta, \theta) d\theta \tag{12}$$

Extending to XFCT. Single angle

First step is considering the case of a fixed angle and inverting the corresponding operator $\mathscr{R}_\gamma$ for a fixed $\gamma \in \Gamma$. The inspiration is the nonrealistic case where $\gamma = \pi$, the exponentials are “parallel“ and the solution of the problem is trivial, just considering $a(x,\theta) = \lambda(x,\theta+\pi) + \mu(x,\theta+\pi)$ and Fokas approach applies in a straightforward manner. This suggests the necessity of considering a rotation of angle γ for the next step towards a generalization.

Extending to XFCT. Single angle. Rotation

For every given point x, the line $\ell(x, v) = \{x + sv : s \geq 0\}$ can be mapped to the line $\ell(x, -v)$ through the rotation operator

$$\phi_x(y) = 2x - y \tag{13}$$

and also can be mapped to the line $\ell(x, G_\gamma v)$ (for a fixed angle γ, being $G_\gamma^T = (\xi_\gamma, \xi_\gamma^\perp)$ a 2x2 rotation matrix) through the following rotation

$$\psi_{\gamma,x}(y) = G_\gamma(y - x) + x. \tag{14}$$

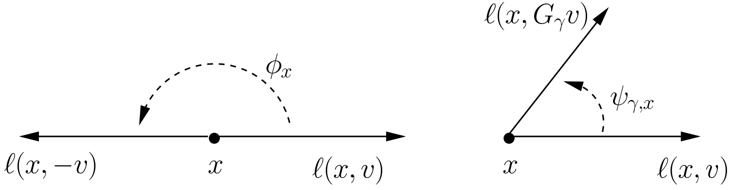

Rotations ϕ_x and $\psi_{\gamma,x}$

The attenuation that we have to consider will be derived from

$$a_{\gamma,x}(y) = \lambda(\phi_x(y)) + b_{\gamma,x}(y) \tag{15}$$

with $b_{\gamma,x}$ a function defined by

$$b_{\gamma,x}(y) = \mu(\psi_{\gamma,x}(y)). \tag{16}$$

And after several lemmas and lots of calculations, we get the inverse $\mathscr{R}_\gamma^{-1}$ for a fixed angle γ.

Series Inversion from the fixed angle approximation

Theorem

If the fluorescence attenuation map μ *satisfies the inequality* $\max_{(x,\theta)} |1 - \alpha(x, \theta, \beta^*)| < 1$, *with* α *defined before, the inverse operator* $\mathscr{R}_{\mathrm{xfct}}^{-1}$ *is given by the Neumann series*

$$\mathscr{R}_{\mathrm{xfct}}^{-1} = \frac{1}{\mathrm{m}} \sum_{k=0}^{\infty} \left(\mathcal{I} - \frac{1}{\mathrm{m}} \mathscr{R}_{\beta^*}^{-1} \mathscr{R}_{\mathrm{xfct}} \right)^k \mathscr{R}_{\beta^*}^{-1} \tag{17}$$

with $\mathcal{I}$ *the identity operator,* $\beta^* = \frac{1}{2}(\gamma_1 + \gamma_2)$, $\mathrm{m} = \gamma_2 - \gamma_1$ *and* $\mathscr{R}_{\beta^*}^{-1}$ *from before.*

In practical experiments, the angle section Γ, is symmetrically chosen to verify $\Gamma \subseteq [0, \pi]$. So, the optimal angle β^* is $\frac{\pi}{2}$ and the condition above is always satisfied since there is a minimum in the amount of scattered photons at $\frac{\pi}{2}$ and therefore the total fluorescence attenuation (the divergent beam transform of μ) is stationary at this angle.

Series Inversion from the fixed angle approximation

Now, using the same change of variables as before, we define the function a, for fixed but arbitrary values of x, by

$$a(x,\eta) = \lambda(\phi_x(x)) + b_{\eta,x}(x), \tag{18}$$

where $x = \phi_x(x)$ and $b = b_{\eta,x}(x)$ such that

$$\mathscr{D} b_{\eta,x}(x,\eta) = -\ln \frac{1}{\mathrm{m}} \int_{\Gamma(x)} e^{-\mathscr{D}\mu(x,G_\gamma \eta)} d\gamma, \tag{19}$$

Since $\mathscr{D}\mu$ is a positive function and $\int_\Gamma d\gamma \; e^{-\mathscr{D}\mu} < \mathrm{m}$, the above logarithm is well defined, i.e., $\mathscr{D} b > 0$.

An Analytic Inverse

If (t, ρ) is the change of variables in $x = t\xi + \rho\xi^{\perp}$, $\mathrm{m} = \gamma_2 - \gamma_1$

$$\omega_{\mathrm{xfct}}(x, \theta) = e^{-\mathcal{D}\lambda(x,\theta+\pi)} \int_{\Gamma} e^{-\mathcal{D}\mu(x,\xi_{\theta+\gamma})} d\gamma.$$

and

$p(t, \theta) = \mathscr{R}\lambda(t, \theta) + \mathscr{R}b(t, \theta)$ and $\mathscr{R}b$ defined by.

$$\mathscr{R}b(x\cdot\xi_\theta, \theta) = -\ln\left[\frac{1}{\mathrm{m}^2}\left(\int_{\Gamma} e^{-\mathcal{D}\mu(x,\theta+\gamma+\pi)} d\gamma\right)\left(\int_{\Gamma} e^{-\mathcal{D}\mu(x,\theta+\gamma)} d\gamma\right)\right].$$

and

$$m\{r, d\} = e^{-\frac{r}{2}}\left\{h_c(r)\mathscr{H}\left(h_c(r)e^{\frac{r}{2}}d\right) + h_s(r)\mathscr{H}\left(h_s(r)e^{\frac{r}{2}}d\right)\right\} \tag{20}$$

with $h_c(r) = \cos(\frac{1}{2}\mathscr{H}r)$ and $h_s(r) = \sin(\frac{1}{2}\mathscr{H}r)$.

An Analytic Inverse: Finally

$$f(x) = \frac{1}{4\pi}\int_0^{2\pi} \partial_t \left[\mathrm{m}\omega_{\mathrm{xfct}}^{-1}(x,\theta) m \left\{ p, \frac{1}{\mathrm{m}}\mathscr{R}_{\mathrm{xfct}} f \right\} (x\cdot\xi,\theta) \right] d\theta \qquad (21)$$

$$= \frac{1}{4\pi}\int_0^{2\pi} \partial_t \left[\omega_{\mathrm{xfct}}^{-1}(x,\theta) m\{p, \mathscr{R}_{\mathrm{xfct}} f\}(x\cdot\xi,\theta) \right] d\theta \qquad (22)$$

$$= \mathscr{R}_{\mathrm{xfct}}^{-1}\mathscr{R}_{\mathrm{xfct}} f(x) \qquad (23)$$

Some Experiments: Simulated Data

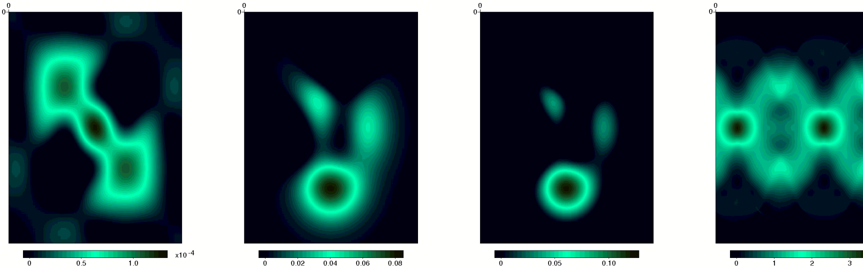

Simulated data: $\{f_1, \lambda_1, \mu_1, \mathscr{R}_{\text{xfct}} f_1\}$, (256×256), sinograms obtained with $M = 360$ views and $N = 400$ rays per view.

Some Experiments: Simulated Data

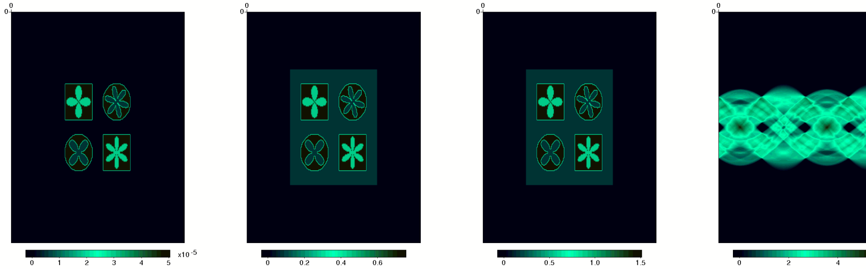

Simulated data: $\{f_2, \lambda_2, \mu_2, \mathscr{R}_{\text{xfct}} f_2\}$, (80×80), sinograms obtained with $M = 360$ views and $N = 400$ rays per view.

Some Experiments: Simulated Data

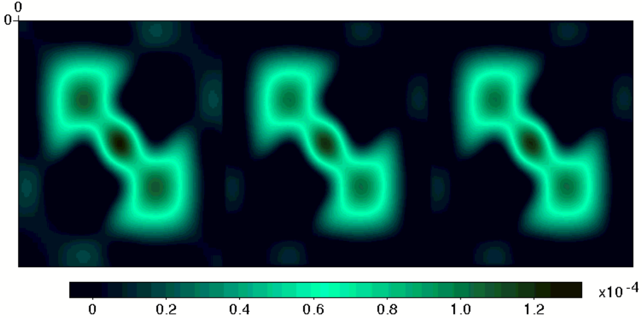

xfct inversion. From left to right: true density map, $\mathscr{R}_{\text{xfct}}^{-1} d$ and $(\text{m}\mathscr{R}_{\beta^*})^{-1} d$ for f_1

Some Experiments: Simulated Data

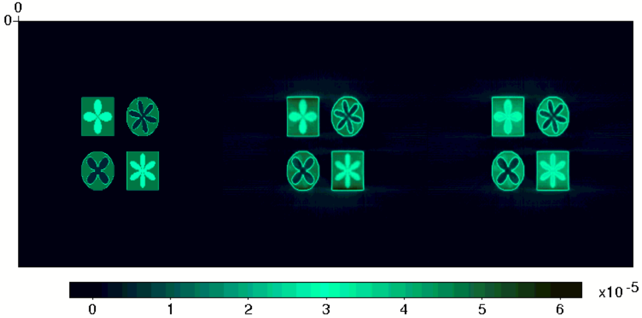

xfct inversion. From left to right: true density map, $\mathscr{R}_{\text{xfct}}^{-1} d$ and $(\text{m}\mathscr{R}_{\beta^*})^{-1} d$ for f_1

Some Experiments: Real Data

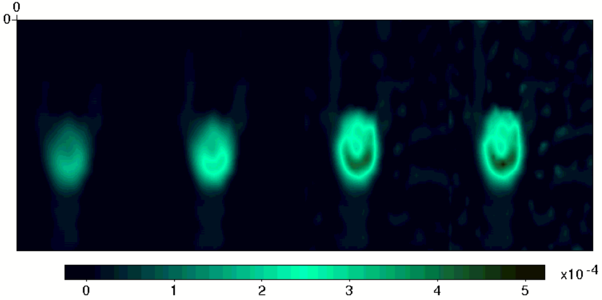

Sequence of partial sums of the approximating series for real data using $\mu = \lambda$.

What is left: Too Many Things

- An extended comparison of all the methods for different types of data (there are many combinations)

What is left: Too Many Things

- An extended comparison of all the methods for different types of data (there are many combinations)
- What is valid for SPECT?

What is left: Too Many Things

- An extended comparison of all the methods for different types of data (there are many combinations)
- What is valid for SPECT?
- A reasonable implementation of the analytic formulas. Better filtering?

What is left: Too Many Things

- An extended comparison of all the methods for different types of data (there are many combinations)
- What is valid for SPECT?
- A reasonable implementation of the analytic formulas. Better filtering?
- 3D?.

What is left: Too Many Things

- An extended comparison of all the methods for different types of data (there are many combinations)
- What is valid for SPECT?
- A reasonable implementation of the analytic formulas. Better filtering?
- 3D?.
- Diffractive data (main direction now)

What is left: Too Many Things

- An extended comparison of all the methods for different types of data (there are many combinations)
- What is valid for SPECT?
- A reasonable implementation of the analytic formulas. Better filtering?
- 3D?.
- Diffractive data (main direction now)
- Etc......

Thanks

The Team

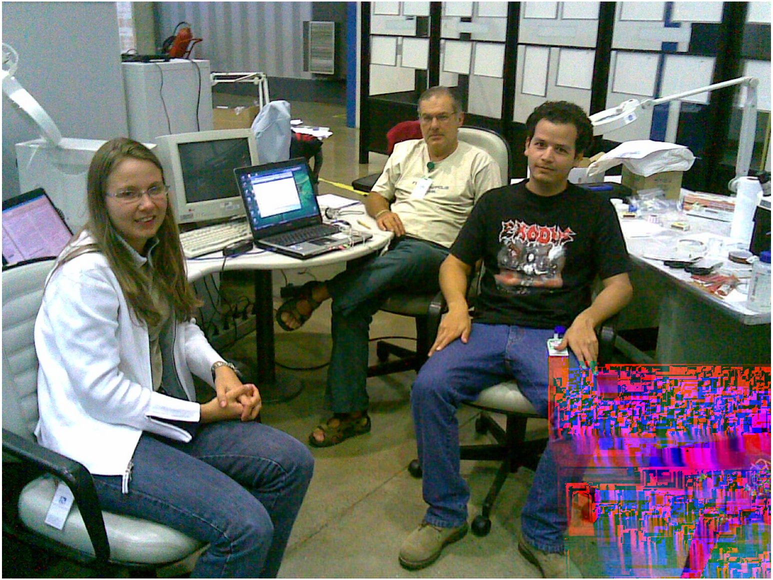

Questions?

Sundown, Uraricoera River, North of the Amazon

Publicity Section

The Huge Conference

Publicity Section

São Paulo - Brazil

Workshop on
Image Processing and Reconstruction: Models and Methods

Part of the International Conference on Mathematical Modeling in Industry

November 30 – December 2, 2011 — USP, São Paulo – Brazil

http://www.lcad.icmc.usp.br/icmmi

From medical applications in diagnosis, going through nondestructive testing, remote sensing, ultramicroscopy, and many others, image reconstruction and processing gives rise to mathematical models and methods associated to some of the most important modern technologies. What these technologies have in common is the fact that they are modeled as inverse and ill-posed problems. These problems are related to different areas, including optimization, computational harmonic analysis, approximation theory and integral equations.

General Talk

Gunther Uhlmann, *Harry Potter's Cloak and Inverse Problems*
University of Washington, Department of Mathematics – USA

Workshop

Andrei Bronnikov, *Mathematics of Phase-Contrast X-Ray Micro-Tomography*
Bronnikov Algorithms – The Netherlands

Ali Mohammad-Djafari, *Sparsity Enforcing Prior Models and Bayesian Approach for Signal and Image Reconstruction*
Laboratoire des Signaux e Systèmes, Univeristé Paris Sud – France

Patrick LaRiviere, *Virtual X-Ray Histology Using Multiple Metal Stains and Multi-Energy Synchrotron microCT*
Dept. of Radiology, University of Chicago Medical Center – USA

Russell Luke, *Imaging from Low-Count X-Ray Diffraction Data: Variational Analysis and Algorithms*
Institut für Numerische und Angewandte Mathematik, Universität Göttingen – Germany

Emil Sidky, *The Role of Compressive Sensing in Iterative Image Reconstruction for Computed Tomography*
Dept. of Radiology, University of Chicago Medical Center – USA

ICMMI

The *International Conference on Mathematical Modeling in Industry* will present over a dozen workshops. For more information, please refer to the website.

Organization

ICMMI
José Alberto Cuminato — SME/ICMC/USP
jacumina@icmc.usp.br

WIPRMM
Elias Salomão Helou — SME/ICMC/USP
elias@icmc.usp.br
Álvaro Rodolfo De Pierro — DMA/IMECC/UNICAMP
alvaro@ime.unicamp.br

The Workshop